Chapter 3

Structure determination of proteins by solid-state MAS NMR

3.1 Introduction

Solid-state MAS NMR spectroscopy is a valuable technique for elucidating the three-dimensional structure of solid proteins. A structural study by NMR encloses two steps. The first step involves the sequence-specific assignment of the chemical shifts. Several multidimensional correlation methods for assigning ^{13}C and ^{15}N resonances have been developed[1-3]. ^{13}C-homonuclear correlation experiments employ either a zero-quantum recoupling sequence such as RFDR[4] or a double-quantum sequence[5-7] such as SPC-5[8] and are important for the identification of the single amino-acid types. Heteronuclear correlation experiments are accomplished with frequency-selective ^{15}N-^{13}C cross-polarization[9] or by using dipolar recoupling techniques such as REDOR[10]. These experiments are essential for connecting the amino-acids in a so-called sequential assignment. Assignment strategies in solid-state MAS NMR are discussed to some extent in Chapter 2. When spectral assignments are complete, the second step of a NMR structural study consists in performing multidimensional experiments to obtain structural restraints, e.g. torsion angles[11-13] and internuclear distances[14-18]. To date, most structural NMR studies of solid proteins relied on preparations with site-specific incorporation of pairs of enriched nuclei, such as ^{13}C-^{13}C and ^{13}C-^{15}N. For such preparations, accurate distances[14-18] and ϕ and ψ backbone torsion angles[11-13] have been determined, with resolution well beyond the one obtainable with x-ray crystallography. This approach has been very successful and will continue to be important to address detailed structural questions in large biomolecular systems[12,18-26].

To efficiently determine the complete fold of a protein, however, it is desirable to incorporate many isotopic labels so that multiple structure restraints can be measured from a small number of samples. The quality of the structure increases with the number of restraints and the more are measured, the lower the accuracy of the individual restraints may be. From a close analysis of the topology of helical and β-sheet structures, it transpires that carbon-carbon distances are very important in defining the fold of a protein. For example, distances between backbone carbons, i.e. alpha and carbonyl carbons, define the secondary structure of a protein. Distances between backbone and side-chain carbons or between side-chain and side-chain carbons provide information about the tertiary structure. Additional restraints can be derived by heteronuclear ^{13}C-^{15}N distances.

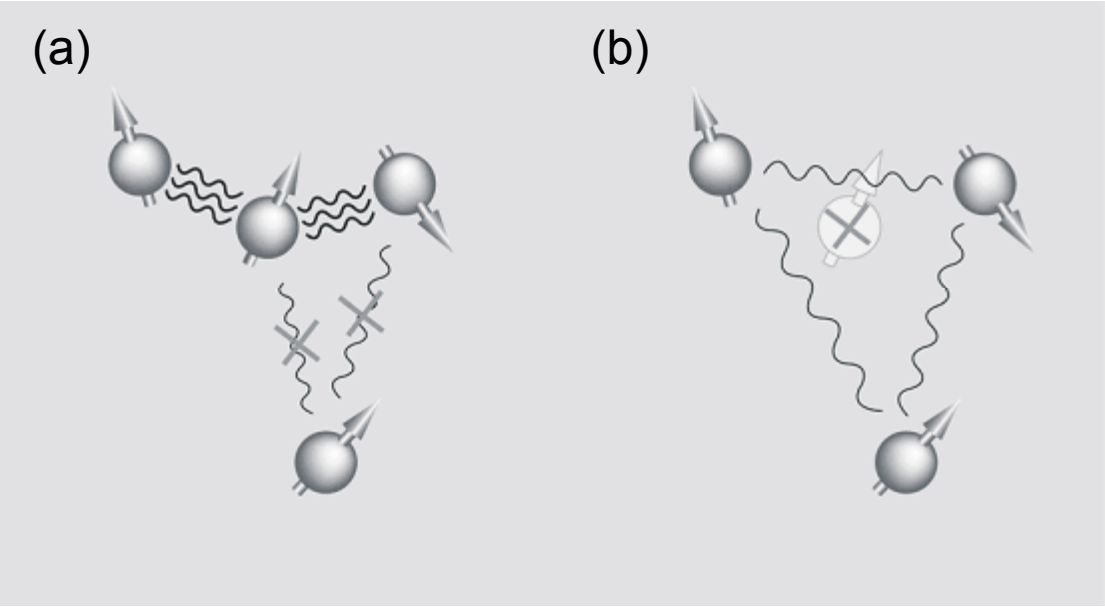

Fig. 3.1 Schematic representation of dipolar truncation mechanisms. (a) The strong dipolar coupling between connect nuclei, do not allow the detection of weak couplings to remote nuclei. (b) By applying spin dilution, the weak couplings, important for structural information, are now detectable.

In uniformly labelled proteins, the measurements of structurally important restraints are complicated by the presence of strong couplings of directly bonded spins. Strong couplings between spins that are close in space prohibit the detection of weak interactions and therefore the measurement of long-range distances, essential for a structure calculation. This effect is referred to as dipolar truncation and is schematically illustrated in Fig. 3.1. In contrast to assignment purposes, where dipolar truncation effects can be disregarded since only one-bond connectivities are required, these effects hamper a straightforward detection of weak long-range correlations. To circumvent the dipolar truncation problem, different approaches have

been developed. One approach involves the application of recoupling techniques that rely on frequency-selective dipolar recoupling schemes. Homonuclear ^{13}C-^{13}C distances can be obtained with spectrally selective methods such as rotational resonance[27], while heteronuclear ^{13}C-^{15}N distances can be measured with frequency-selective REDOR experiments[28]. Recently modified 3D TEDOR experiments have been designed, to simultaneously measure multiple long-range nitrogen-carbon distances in uniformly ^{13}C,^{15}N-labelled samples[29]. Other methods are based on experiments for torsion-angle determination, applicable on uniformly labelled systems[11,30-34]. A second approach to suppress dipolar truncation effects relies on combining broad-band recoupling methods with dilution of ^{13}C spins. Spin dilution reduces or completely removes the number of directly connected ^{13}C nuclei and hence of most of the strong couplings in the system. Therefore, weak couplings between remote spins can be detected and used as structural restraints. We have followed the second approach, which combines spin diffusion experiments with dilution of ^{13}C spins, allowing the detection of a large number of low-accuracy ^{13}C-^{13}C distances for structure calculations, as described in Section 3.3. In the next Section, an analysis of carbon-carbon distances in the most commonly encountered secondary structures of proteins in the 2-7 Å range is presented.

3.2 Structure defining ^{13}C-^{13}C distances in proteins

For structure determination, a large number of distances in the 2–7 Å range are needed. Different types of carbon-carbon distances can be taken into account to define the three-dimensional structure of α-helical and β-sheet proteins. Tab. 3.1 gives average values plus variation for some of these distances. The distances were derived from a set of structures, which contain the different types of secondary structure elements, as depicted in Fig. 3.2.

In α-helices, distances between backbone carbons of residues i and i+n (n= 1,..4) are the shortest and most characteristic for defining this type of secondary structure. Magnetization transfer between C^{α}_{i}-$CO_{i+2,3}$ covers distances of the order of 5.5 ±0.2 Å and should lead to small, but detectable cross peaks in carbon-carbon correlation spectra. Distances of the type C^{α}_{i}-CO_{i+4} are around 7 Å and should not necessarily be observable. The CO_i-$C^{\alpha}_{i+2,3,4}$ distances are in the range of 4.3 to 4.9 Å and hence valuable as well for defining the α-helical structure. For distances between different C^{α}, the C^{α}_{i}-C^{α}_{i+3} is always the shortest and together

with CO_i-$CO_{i+2,3}$ distances most indicative of the α-helix. The distances between the backbone carbons i and the $C^{\beta}_{i+2,3}$ are also short enough to expect detectable cross-peaks.

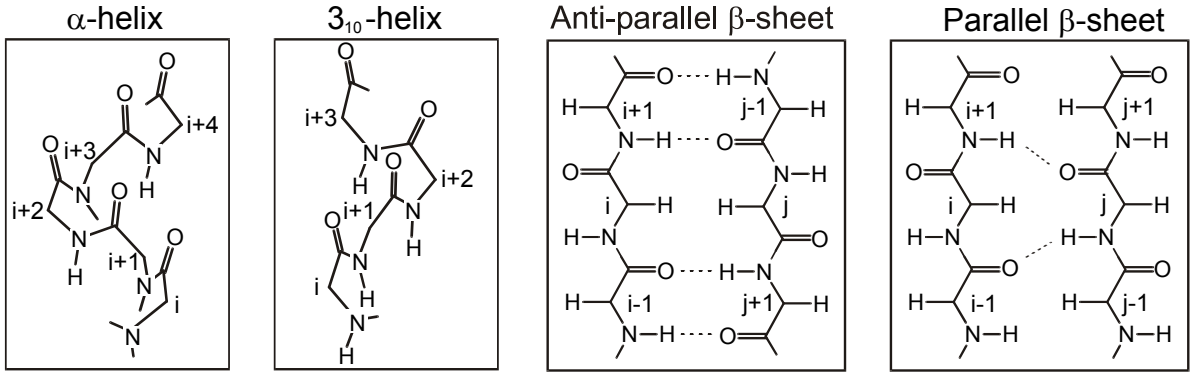

Fig. 3.2 Schematic representation of α-helix, 3_{10}-helix, anti-parallel β-sheet and parallel β-sheet secondary structure motives. The numbering of the residues (i and j) corresponds to the numbering in Tab. 3.1.

Structure-defining ^{13}C-^{13}C distances in proteins

Secondary structure	residue	C^{α}-C^{α} (Å)	CO-CO (Å)	C^{α}-CO (Å)	CO-C^{α} (Å)	C^{α}-C^{β} (Å)	CO-C^{β} (Å)
α-helix	i,i+1	3.8 ±0.1	3.0 ±0.1	4.4 ±0.1	2.4 ±0.1	4.9 ±0.1	3.7 ±0.1
	i,i+2	5.5 ±0.3	4.5 ±0.1	5.4 ±0.2	4.4 ±0.2	6.0 ±0.5	5.2 ±0.3
	i,i+3	5.0 ±0.2	4.7 ±0.1	5.5 ±0.2	4.4 ±0.2	4.4 ±0.5	4.3 ±0.4
	i,i+4	6.0 ±0.2	5.9 ±0.2	7.2 ±0.2	4.9 ±0.2	5.7 ±0.5	4.5 ±0.3
3_{10}-helix	i,i+1	3.8 ±0.1	3.1 ±0.2	4.5 ±0.2	2.4 ±0.1	4.9 ±0.1	3.7 ±0.1
	i,i+2	5.3 ±0.3	4.6 ±0.2	5.6 ±0.2	4.3 ±0.3	5.6 ±0.5	5.0 ±0.5
	i,i+3	5.6 ±0.4	5.5 ±0.3	6.6 ±0.5	4.7 ±0.3	5.0 ±0.5	4.5 ±0.5
	i,i+4	8.1 ±0.4	7.9 ±0.4	9.2 ±0.5	6.8 ±0.4	8.3 ±0.5	6.9 ±0.5
Anti-parallel β-sheet	i,j	4.6 ±0.3		5.4 ±0.5		5.4 ±0.7	
	i-1,j+1	5.4 ±0.3	5.0 ±0.4				
	i-1,j		4.9 ±0.3		4.7 ±0.5		5.4 ±0.7
Parallel β-sheet	i,j	4.9 ±0.5	4.9 ±0.3	4.6 ±0.6	5.6 ±0.3	4.6 ±0.6	5.6 ±0.7

Tab. 3.1 Summary of the most characteristic, structure-defining ^{13}C-^{13}C distances in proteins. The four most commonly encountered secondary structure motifs are considered. For each secondary structure element, a set of structures was selected and distances between backbone-backbone and backbone side-chain carbons were measured. The errors are estimated from the dispersion of the distances in the selected structures. The indices of the residues refer to the schematic representation of secondary structures shown in Fig. 3.2.

The characteristic feature of a 3_{10}-helix is that this secondary structure motif is more elongated than an α-helix. For the 3_{10}-helix, distances between backbone carbons of residues i and i+4 are generally too long to provide detectable cross-peaks. Stronger cross-peaks are expected for correlations between CO_i-CO_{i+2} and CO_i-$C^{\alpha}_{i+2,3}$, due to transfer over distances in the 4.3–4.7 Å range. Weaker but still detectable peaks may occur because of correlations of

the type C^{α}-CO of residues i and i+2, i+3. Also important for defining the 3_{10}-helix are correlations between the backbone carbons i and side-chains $C^{\beta}_{i+2,3}$.

In contrast to helices, β-sheet topologies are mostly defined by contacts between backbone carbons located in different strands (see Fig. 3.2). In the case of an anti-parallel β-sheet, we have indicated with i and j the residues of different strands that have the C^{α} closer together, and with i+1 and j-1 the residues which have the C^{α} further apart (Fig. 3.2). The C^{α}_{i}-C^{α}_{j} distances are relatively short, 4.6 ± 0.3 Å, while those between C^{α}_{i+1} and C^{α}_{j-1} are of the order of 5.4 ± 0.3 Å. The shortest distances between carbonyl carbons are found for residues i and j+1, and i−1and j, and are of the order of 5.0± 0.4 Å. Distances of the type C^{α}_{i}-CO_{j+1} are about 5.4 ± 0.5 Å and those of the type CO_{i-1}-C^{α}_{j} about 4.7 ± 0.5 Å. The latter are very valuable for defining anti-parallel β-sheet secondary structure. Cross-peaks may also be observed between backbone carbons of one strand and the β-carbons of a neighbouring strand. The shortest distances of this type are of the order of 5.4 ± 0.7 Å. In the case of a parallel β-sheet, we define i and j as the closest residues located in the two parallel strands. All the distances between backbone carbons are in range of 4.6 to 5.6 Å and should give rise to detectable signals. In the same range are the distances between backbone carbons and β-carbons.

3.3 Our approach: broad-band recoupling method and spin dilution

To be able to determine the structure of proteins by solid-state MAS NMR, we developed a methodology that is based on the detection of a large number of ^{13}C-^{13}C structure-defining distances from a small number of samples, with minimal experimental effort. In a uniformly labelled preparation, the detection of long-range carbon-carbon restraints is obscured by the strong coupling of directly bonded ^{13}C spins. This occurs because of dipolar truncation effects[35-37] (see Fig. 3.1). By employing a reduced labelling scheme, in which chemically-bonded carbons are mostly not simultaneously labelled and hence the number of strong dipolar couplings between connected nuclei is reduced, we were able to detect weak couplings that contained the structural information of interest. For proteins expressed in bacterial systems, a reduced ^{13}C-labelling can be achieved by using [2-^{13}C] glycerol or [1,3-^{13}C] glycerol, as the sole carbon source in the media[36,38,39] (see Chapter 4). The result is an

almost alternating labelling scheme, where still many carbon sites are labelled but not in adjacent positions.

In combination with this labelling pattern, long-range ^{13}C-^{13}C distance restraints may be collected by using a simple broad-band recoupling method like the proton-driven spin diffusion (PDSD) mixing scheme[40] (see Chapter 5). In Fig. 3.3 the pulse-sequence of the standard 2D PDSD experiment is shown. The advantages of this technique are its robustness owing to its simplicity and aptness to be implemented for very long mixing times. Typically, mixing times of 500 ms for ^{13}C-^{13}C spectra and of several seconds for ^{15}N-^{15}N spectra can be used, without limitations on balancing radio-frequency power input and sample heating.

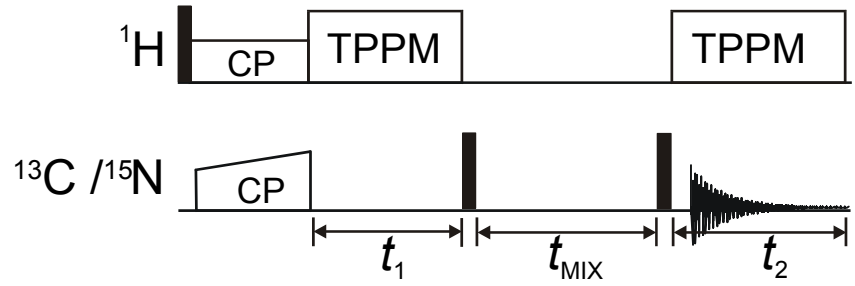

Fig. 3.3 Pulse program of a standard 2D homonuclear PDSD dipolar correlation experiment, applicable in the case of ^{13}C-^{13}C or ^{15}N-^{15}N correlation spectra. Following ^{1}H excitation, a ramped cross-polarization between ^{1}H and ^{15}N or ^{13}C creates the initial $^{15}N/^{13}C$ magnetization. Following the nitrogen or carbon evolution, a 90º pulse on the low-γ nucleus brings back the magnetization along the z-axis. During the mixing time t_{MIX}, proton decoupling is switched off and the polarization transfer between ^{15}N or ^{13}C spins occur in the presence of ^{1}H-^{1}H and ^{1}H-^{15}N (or ^{1}H-^{13}C) dipolar couplings. During all evolution periods, proton decoupling is applied, using the two-pulse phase modulation technique (TPPM).

The long-range correlations can be assigned and the distance restraints for the structure calculation can be obtained by looking at the initial build-up rates of these correlations, as explained in detail in Chapter 5. The relatively low-accuracy of these distance restraints is compensated by their high amount.

As will be demonstrated in Chapter 5 and 6, this approach leads to a sufficiently large set of long-range distance restraints to calculate the structure of a protein. We believe that this strategy can be applicable to a wide range of bacterial membrane proteins in the solid state and for the study of receptor-bound agonists and antagonists. The dataset may be supplemented by ^{1}H-^{1}H restraints obtained from proton-proton correlation spectroscopy using samples deuterated at non-exchangeable sites[41-43] or by ^{13}C-^{15}N restraints from C-N dipolar correlation spectroscopy using doubly-labelled samples.

References

1. Detken, A., Hardy, E. H., Ernst, M., Kainosho, M., Kawakami, T., Aimoto, S., & Meier, B. H. (2001). Methods for sequential resonance assignment in solid, uniformly 13C, 15N labelled peptides: quantification and application to antamanide. *J. Biomol. NMR* **20**, 203-221.

2. Pauli, J., Baldus, M., van Rossum, B., de Groot, H., & Oschkinat, H. (2001). Backbone and side-chain C-13 and N-15 signal assignments of the alpha-spectrin SH3 domain by magic angle spinning solid-state NMR at 17.6 tesla. *Chembiochem* **2**, 272-281.

3. Rienstra, C. M., Hohwy, M., Hong, M., & Griffin, R. G. (2000). 2D and 3D N-15-C-13-C-13 NMR chemical shift correlation spectroscopy of solids: Assignment of MAS spectra of peptides. *J. Am. Chem. Soc.* **122**, 10979-10990.

4. Bennett, A. E., Ok, J. H., Griffin, R. G., & Vega, S. (1992). Chemical-Shift Correlation Spectroscopy in Rotating Solids - Radio Frequency-Driven Dipolar Recoupling and Longitudinal Exchange. *J. Chem. Phys.* **96**, 8624-8627.

5. Lee, M. & Goldburg, W. I. (1965). Nuclear Magnetic Resonance Line Narrowing by a Rotating RF Field. *Phys. Rev. A* **140**, 1261-1271.

6. Sun, B. Q., Costa, P. R., Kocisko, D., Lansbury, P. T., & Griffin, R. G. (1995). Internuclear Distance Measurements in Solid-State Nuclear-Magnetic-Resonance - Dipolar Recoupling Via Rotor Synchronized Spin Locking. *J. Chem. Phys.* **102**, 702-707.

7. Nielsen, N. C., Bildsoe, H., Jakobsen, H. J., & Levitt, M. H. (1994). Double-Quantum Homonuclear Rotary Resonance - Efficient Dipolar Recovery in Magic-Angle-Spinning Nuclear-Magnetic-Resonance. *J. Chem. Phys.* **101**, 1805-1812.

8. Hohwy, M., Rienstra, C. M., Jaroniec, C. P., & Griffin, R. G. (1999). Fivefold symmetric homonuclear dipolar recoupling in rotating solids: Application to double quantum spectroscopy. *J. Chem. Phys.* **110**, 7983-7992.

9. Baldus, M., Petkova, A. T., Herzfeld, J., & Griffin, R. G. (1998). Cross polarization in the tilted frame: assignment and spectral simplification in heteronuclear spin systems. *Mol. Phys.* **95**, 1197-1207.

10. Gullion, T. & Schaefer, J. (1989). Rotational-Echo Double-Resonance Nmr. *J. Magn. Reson.* **81**, 196-200.

11. Feng, X., Verdegem, P. J. E., Lee, Y. K., Sandstrom, D., Eden, M., BoveeGeurts, P., deGrip, W. J., Lugtenburg, J., deGroot, H. J. M., & Levitt, M. H. (1997). Direct determination of a molecular torsional angle in the membrane protein rhodopsin by solid-state NMR. *J. Am. Chem. Soc.* **119**, 6853-6857.

12. Feng, X., Verdegem, P. J. E., Eden, M., Sandstrom, D., Lee, Y. K., Bovee-Geurts, P. H. M., de Grip, W. J., Lugtenburg, J., de Groot, H. J. M., & Levitt, M. H. (2000). Determination of a molecular torsional angle in the metarhodopsin-I photointermediate of rhodopsin by double-quantum solid-state NMR. *J. Biomol. NMR* **16**, 1-8.

13. Bower, P. V., Oyler, N., Mehta, M. A., Long, J. R., Stayton, P. S., & Drobny, G. P. (1999). Determination of torsion angles in proteins and peptides using solid state NMR. *J. Am. Chem. Soc.* **121**, 8373-8375.

14. Benzinger, T. L., Gregory, D. M., Burkoth, T. S., Miller-Auer, H., Lynn, D. G., Botto, R. E., & Meredith, S. C. (1998). Propagating structure of Alzheimer's beta-amyloid(10-35) is parallel beta-sheet with residues in exact register. *Proc. Natl. Acad. Sci. U. S. A* **95**, 13407-13412.

15. Creuzet, F., McDermott, A., Gebhard, R., vanderHoef, K., Spijkerassink, M. B., Herzfeld, J., Lugtenburg, J., Levitt, M. H., & Griffin, R. G. (1991). Determination of Membrane-Protein Structure by Rotational Resonance Nmr - Bacteriorhodopsin. *Science* **251**, 783-786.

16. Griffiths, J. M., Lakshmi, K. V., Bennett, A. E., Raap, J., Vanderwielen, C. M., Lugtenburg, J., Herzfeld, J., & Griffin, R. G. (1994). Dipolar Correlation Nmr-Spectroscopy of A Membrane-Protein. *J. Am. Chem. Soc.* **116**, 10178-10181.

17. Klug, C. A., Tasaki, K., Tjandra, N., Ho, C., & Schaefer, J. (1997). Closed form of liganded glutamine-binding protein by rotational-echo double-resonance NMR. *Biochemistry* **36**, 9405-9408.

18. Verdegem, P. J. E., Helmle, M., Lugtenburg, J., & deGroot, H. J. M. (1997). Internuclear distance measurements up to 0.44 nm for retinals in the solid state with 1-D rotational resonance C-13 MAS NMR spectroscopy. *J. Am. Chem. Soc.* **119**, 169-174.

19. Balbach, J. J., Petkova, A. T., Oyler, N. A., Antzutkin, O. N., Gordon, D. J., Meredith, S. C., & Tycko, R. (2002). Supramolecular structure in full-length Alzheimer's beta-amyloid fibrils: evidence for a parallel beta-sheet organization from solid-state nuclear magnetic resonance. *Biophys. J.* **83**, 1205-1216.

20. Isaac, B., Gallagher, G. J., Balazs, Y. S., & Thompson, L. K. (2002). Site-directed rotational resonance solid-state NMR distance measurements probe structure and mechanism in the transmembrane domain of the serine bacterial chemoreceptor. *Biochemistry* **41**, 3025-3036.

21. Smith, S. O., Eilers, M., Song, D., Crocker, E., Ying, W., Groesbeek, M., Metz, G., Ziliox, M., & Aimoto, S. (2002). Implications of threonine hydrogen bonding in the glycophorin A transmembrane helix dimer. *Biophys. J.* **82**, 2476-2486.

22. Blanco, F. J., Hess, S., Pannell, L. K., Rizzo, N. W., & Tycko, R. (2001). Solid-state NMR data support a helix-loop-helix structural model for the N-terminal half of HIV-1 Rev in fibrillar form. *J. Mol. Biol.* **313**, 845-859.

23. Jaroniec, C. P., MacPhee, C. E., Astrof, N. S., Dobson, C. M., & Griffin, R. G. (2002). Molecular conformation of a peptide fragment of transthyretin in an amyloid fibril. *Proc. Natl. Acad. Sci. U. S. A* **99**, 16748-16753.

24. Nishimura, K., Kim, S., Zhang, L., & Cross, T. A. (2002). The closed state of a H+ channel helical bundle combining precise orientational and distance restraints from solid state NMR. *Biochemistry* **41**, 13170-13177.

25. Petkova, A. T., Hatanaka, M., Jaroniec, C. P., Hu, J. G. G., Belenky, M., Verhoeven, M., Lugtenburg, J., Griffin, R. G., & Herzfeld, J. (2002). Tryptophan interactions in

bacteriorhodopsin: A heteronuclear solid-state NMR study. *Biochemistry* **41**, 2429-2437.

26. van Beek, J. D., Hess, S., Vollrath, F., & Meier, B. H. (2002). The molecular structure of spider dragline silk: folding and orientation of the protein backbone. *Proc. Natl. Acad. Sci. U. S. A* **99**, 10266-10271.

27. Raleigh, D. P., Levitt, M. H., & Griffin, R. G. (1988). Rotational Resonance in Solid-State Nmr. *Chem. Phys. Lett.* **146**, 71-76.

28. Jaroniec, C. P., Tounge, B. A., Herzfeld, J., & Griffin, R. G. (2001). Frequency selective heteronuclear dipolar recoupling in rotating solids: accurate (13)C-(15)N distance measurements in uniformly (13)C,(15)N-labeled peptides. *J. Am. Chem. Soc.* **123**, 3507-3519.

29. Jaroniec, C. P., Filip, C., & Griffin, R. G. (2002). 3D TEDOR NMR experiments for the simultaneous measurement of multiple carbon-nitrogen distances in uniformly C-13, N-15-labeled solids. *J. Am. Chem. Soc.* **124**, 10728-10742.

30. Costa, P. R., Gross, J. D., Hong, M., & Griffin, R. G. (1997). Solid-state NMR measurement of Psi in peptides: a NCCN 2Q-heteronuclear local field experiment. *Chem. Phys. Lett.* **280**, 95-103.

31. Feng, X., Lee, Y. K., Sandstrom, D., Eden, M., Maisel, H., Sebald, A., & Levitt, M. H. (1996). Direct determination of a molecular torsional angle by solid-state NMR. *Chem. Phys. Lett.* **257**, 314-320.

32. Ladizhansky, V., Veshtort, M., & Griffin, R. G. (2002). NMR determination of the torsion angle Psi in alpha-helical peptides and proteins: The HCCN dipolar correlation experiment. *J. Magn. Reson.* **154**, 317-324.

33. Rienstra, C. M., Hohwy, M., Mueller, L. J., Jaroniec, C. P., Reif, B., & Griffin, R. G. (2002). Determination of multiple torsion-angle constraints in U-C-13,N-15-labeled peptides: 3D H-1-N-15-C-13-H-1 dipolar chemical shift NMR spectroscopy in rotating solids. *J. Am. Chem. Soc.* **124**, 11908-11922.

34. Ladizhansky, V., Jaroniec, C. P., Diehl, A., Oschkinat, H., & Griffin, R. G. (2003). Measurement of multiple psi torsion angles in uniformly 13C,15N-labeled alpha-spectrin SH3 domain using 3D 15N-13C-13C-15N MAS dipolar-chemical shift correlation spectroscopy. *J. Am. Chem. Soc.* **125**, 6827-6833.

35. Hodgkinson, P. & Emsley, L. (1999). The accuracy of distance measurements in solid-state NMR. *J. Magn. Reson.* **139**, 46-59.

36. Hong, M. & Jakes, K. (1999). Selective and extensive 13C labeling of a membrane protein for solid-state NMR investigations. *J. Biomol. NMR* **14**, 71-74.

37. Kiihne, S., Mehta, M. A., Stringer, J. A., Gregory, D. M., Shiels, J. C., & Drobny, G. P. (1998). Distance measurements by dipolar recoupling two-dimensional solid-state NMR. *Journal of Physical Chemistry A* **102**, 2274-2282.

38. LeMaster, D. M. & Kushlan, D. M. (1996). Dynamical mapping of E-coli thioredoxin via C-13 NMR relaxation analysis. *J. Am. Chem. Soc.* **118**, 9255-9264.

39. Hong, M. (1999). Determination of multiple ***φ***-torsion angles in proteins by selective and extensive (13)C labeling and two-dimensional solid-state NMR. *J. Magn Reson.* **139**, 389-401.

40. Szeverenyi, N. M., Sullivan, M. J., & Maciel, G. E. (1982). Observation of Spin Exchange by Two-Dimensional Fourier-Transform C-13 Cross Polarization-Magic-Angle Spinning. *J. Magn. Reson.* **47**, 462-475.

41. Brown, S. P. & Spiess, H. W. (2001). Advanced solid-state NMR methods for the elucidation of structure and dynamics of molecular, macromolecular, and supramolecular systems. *Chem. Rev.* **101**, 4125-4156.

42. Reif, B., Jaroniec, C. P., Rienstra, C. M., Hohwy, M., & Griffin, R. G. (2001). 1H-1H MAS correlation spectroscopy and distance measurements in a deuterated peptide. *J. Magn Reson.* **151**, 320-327.

43. Reif, B., van Rossum, B. J., Castellani, F., Rehbein, K., Diehl, A., & Oschkinat, H. (2003). Characterization of (1)H-(1)H Distances in a Uniformly (2)H,(15)N-Labeled SH3 Domain by MAS Solid-State NMR Spectroscopy(section sign). *J. Am. Chem. Soc.* **125**, 1488-1489.